

Majorana ensembles with fractional entropy and conductance in nanoscopic systems

Sergey Smirnov

*P. N. Lebedev Physical Institute of the Russian Academy of Sciences, 119991 Moscow, Russia**

(Dated: November 12, 2021)

Quantum thermodynamics is a promising route to unambiguous detections of Majorana bound states. Being fundamentally different from quantum transport, this approach reveals unique Majorana thermodynamic behavior and deepens our insight into Majorana quantum transport itself. Here we demonstrate that a nanoscopic system with topological superconductors produces a remarkable accumulation of Majorana thermodynamic states in wide ranges of Majorana tunneling phases by means of increasing its temperature T . Revealing this physical behavior is twofold beneficial. First, it significantly reduces the dependence of the entropy on the tunneling phases which become almost irrelevant in experiments. Second, the fractional Majorana entropy $S_M^{(2)} = k_B \ln(2^{\frac{3}{2}})$ may be observed at high temperatures substantially facilitating experiments. Analyzing quantum transport, we predict that when the temperature increases, the above thermodynamic behavior will induce an anomalous increase of the linear conductance from vanishing values up to the unitary fractional Majorana plateau $G_M = e^2/2h$ extending to high temperatures.

I. INTRODUCTION

Non-Abelian Majorana [1] bound states (MBSs) are promising candidates for topological fault-tolerant quantum computation [2, 3]. While theoretically MBSs are assumed to exist in topological superconductors (TSs) [4–8], their conclusive detection is a challenge. A possible experimental platform for fully conclusive Majorana signatures is quantum transport and the most direct observable is the electric conductance. Recently there have appeared critique [9, 10] of numerous experiments on average electric currents to detect MBSs. Thus a crisis in measurements of the Majorana conductance is evident. Nevertheless, the quantum transport potential remains far from being exhausted, awaiting its soon implementation for various detections of MBSs. For instance, shot noise [11–13] is a promising route because it explicitly reveals [14] a fractionalization of Dirac fermions with the integer charge e into well separated MBSs with the fractional effective charge $e/2$. Further, finite frequency noise [15] or quantum noise [16] detects MBSs via finite frequency resonances with fractional maxima. More comprehensive experiments involve thermoelectric currents [17–20], universal Majorana thermoelectric noise [21], Majorana thermoelectric quantum noise at finite frequencies [22], combinations of thermal nonequilibrium with thermodynamic properties [23] and Majorana dynamics of other observables such as magnetization [24].

A fundamentally different way to unambiguously observe MBSs is quantum thermodynamics, in particular, measurements of the entropy of a mesoscopic system. Whereas the value of the Majorana conductance may result from other physical phenomena totally unrelated to MBSs, measuring a fractional Majorana en-

tropy $S_M = k_B \ln(2^{\frac{n}{2}})$, where n is an odd positive integer, $n = 1, 3, 5, \dots$, unambiguously signals [25] that the system hosts well separated halves of Dirac fermions. Indeed, all topologically trivial zero energy bound states have an integer entropy $S_n = k_B \ln(2^n)$, where n is an integer, $n = 0, 1, 2, \dots$, and thus such states are unambiguously filtered out as having nothing to do with MBSs. Recent experiments and experimental proposals on the entropy in mesoscopic systems [26–30] demonstrate that Majorana entropy measurements [31] are feasible. However, as shown in Ref. [32], difficulties arise due to the sensitivity of the entropy to tunneling phases emerging in realistic setups with possible interference effects [33]. Although in a particular setup one may try to prepare TSs long enough to reduce effects of the Majorana tunneling phases, in practical applications these phases cannot be removed and are fundamentally used for a proper control of Majorana qubits [34, 35]. More crucially, experimental observations of the Majorana entropy require very low temperatures which are hard to achieve.

Here we reveal a remarkable property of a system with MBSs to accumulate Majorana thermodynamic states (or ensemble states) in wide ranges of tunneling phases when the system's temperature is increased. This surprisingly solves the two difficulties above: it significantly diminishes dependence of the entropy on Majorana tunneling phases and at the same time substantially increases the temperatures at which the Majorana entropy may be measured in realistic setups of practical significance. Moreover, we demonstrate that involving more than two MBSs essentially simplifies experiments because it fully eliminates sensitive adjustments between the tunneling phases and gate voltage [32]. Crucially for quantum transport experiments, we predict that the emergence of these Majorana thermodynamic states leads to an anomalous behavior of the linear conductance. Specifically, instead of a commonly expected suppression of a unitary conductance maximum to vanishing values, increasing the system's temperature induces here a remarkable growth of the linear conductance from vanish-

* 1) sergej.physik@gmail.com

2) sergey.smirnov@physik.uni-regensburg.de

3) ssmirnov@sci.lebedev.ru

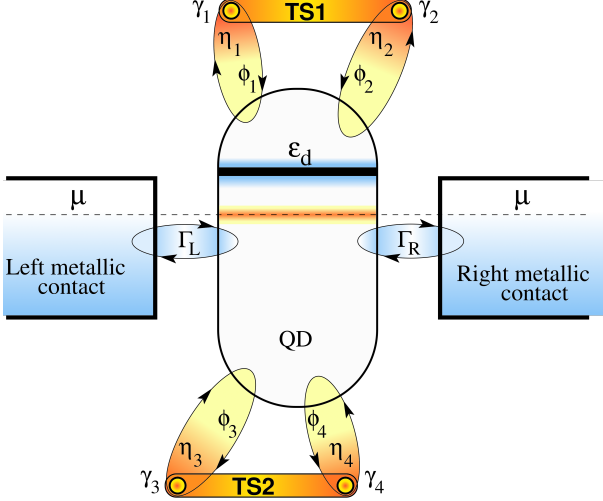


FIG. 1. Outline of a quantum device revealing unique Majorana thermodynamic and transport behavior.

ing values up to the unitary fractional Majorana plateau $G_M = e^2/2h$ extending to high temperatures. Therefore, besides the fractional Majorana entropy, such anomalous behavior of the linear conductance is a fully conclusive signature of MBSs in quantum transport experiments performed in the same setup. An apparent feasibility to detect MBSs at high temperatures by means of measuring the entropy, linear conductance or their mutual behavior in a single mesoscopic setup is very attractive for contemporary experiments.

The paper is organized as follows. Section II describes a Majorana setup, its theoretical model and the expressions for the entropy and linear conductance in terms of the quantum dot Green's functions. The expressions for the Green's functions are also provided. In Section III we show how the entropy depends on the tunneling phases at low and high temperatures, demonstrate the Majorana universality of the entropy and linear conductance and explore their temperature dependence at different values of the tunneling phases. Finally, Section IV concludes the paper and presents possible outlooks.

II. MAJORANA SETUP, ENTROPY AND LINEAR CONDUCTANCE

To explore quantum thermodynamic and transport signatures of MBSs we consider the physical setup shown in Fig. 1. The device represents an essential part of a Majorana qubit and involves a quantum dot (QD), two metallic contacts and two grounded TSs, labeled as TS1 and TS2. Both TS1 and TS2 support MBSs at their ends, $\gamma_{1,2}$ and $\gamma_{3,4}$, respectively. The entanglement of the QD states with the quantum states of the two metallic contacts and two TSs is designed and controlled via inducing tunneling interactions indicated schematically by the corresponding

ellipses with arrows. The four MBSs $\gamma_{1,2,3,4}$ are in general all involved in the tunneling interactions between QD and TSs with, respectively, the tunneling amplitudes $|\eta_{1,2,3,4}|$ and phases $\phi_{1,2,3,4}$. The total Hamiltonian of this system is $\hat{H} = \hat{H}_D + \hat{H}_C + \hat{H}_{TS} + \hat{H}_{NT} + \hat{H}_{MT}$, where the Hamiltonians of the QD, contacts and their tunneling coupling describe the normal part of the system,

$$\begin{aligned}\hat{H}_D &= \epsilon_d d^\dagger d, \\ \hat{H}_C &= \sum_{l=L,R} \sum_k \epsilon_k c_{lk}^\dagger c_{lk}, \\ \hat{H}_{NT} &= \sum_{l=L,R} \tau_l \sum_k c_{lk}^\dagger d + \text{H.c.}\end{aligned}\quad (1)$$

The energy level ϵ_d may be tuned with respect to the chemical potential by a gate voltage. In particular, using $\epsilon_d \geq 0$ excludes possible Kondo universality [36–38] and reveals Majorana universal behavior. The contacts' density of states $\nu_c/2$ specifies the tunneling coupling, $\Gamma \equiv \sum_{l=L,R} \Gamma_l$, $\Gamma_l \equiv \pi \nu_c |\tau_l|^2$. The Majorana part is

$$\begin{aligned}\hat{H}_{TS} &= i(\xi_{12}\gamma_2\gamma_1 + \xi_{34}\gamma_4\gamma_3)/2, \\ \hat{H}_{MT} &= \eta_1^\dagger d^\dagger \gamma_1 + \eta_2^\dagger d^\dagger \gamma_2 + \eta_3^\dagger d^\dagger \gamma_3 + \eta_4^\dagger d^\dagger \gamma_4 + \text{H.c.},\end{aligned}\quad (2)$$

where $\gamma_k^\dagger = \gamma_k$, $\{\gamma_k, \gamma_l\} = 2\delta_{kl}$, $\eta_k = |\eta_k| \exp(i\phi_k)$, $k, l = 1, 2, 3, 4$, and ξ_{12}, ξ_{34} are the energies characterizing the MBSs overlap in TS1 and TS2. Although there are four tunneling phases, physical observables must depend only on three tunneling phase differences, *e.g.*, on

$$\Delta\phi_{1k} \equiv \phi_1 - \phi_k, \quad k = 2, 3, 4. \quad (3)$$

It is important to note that, as mentioned in the introduction, one may prepare TS1 and TS2 long enough so that, *e.g.*, $|\eta_{2,4}|$ become sufficiently small and physical observables become independent of $\Delta\phi_{12}$ and $\Delta\phi_{14}$. However, since the couplings $|\eta_{1,3}|$ are finite, the phase difference $\Delta\phi_{13}$ is fundamentally present and even necessary for quantum computing using Majorana qubits [34, 35] whose initialization in a proper Majorana equilibrium state may be specified by a suitable fractional value of the entropy tuned by $\Delta\phi_{1k}$.

The entropy S is found as the derivative $S = -\partial\Omega/\partial T$ of the system's thermodynamic potential $\Omega = -k_B T \ln Z$ over the temperature T . As in Refs. [25, 32], the thermodynamic partition function Z may be derived from a skew-symmetric imaginary time field integral [39] over the antiperiodic Grassmann fields corresponding to the creation and annihilation operators in \hat{H}_D , \hat{H}_C and \hat{H}_{TS} . The general expression for the entropy of a system with TSs supporting MBSs has been derived in Ref. [25]. It has the following form:

$$\begin{aligned}S &= k_B \ln \left[\cosh \left(\frac{\xi_{12}}{2k_B T} \right) \right] - \frac{\xi_{12}}{2T} \tanh \left(\frac{\xi_{12}}{2k_B T} \right) \\ &+ k_B \ln \left[\cosh \left(\frac{\xi_{34}}{2k_B T} \right) \right] - \frac{\xi_{34}}{2T} \tanh \left(\frac{\xi_{34}}{2k_B T} \right) \\ &+ k_B 2 \ln(2) + \frac{1}{8\pi k_B T^2} \int_{-\infty}^{\infty} d\epsilon \frac{\epsilon \phi(\epsilon)}{\cosh^2 \left(\frac{\epsilon}{2k_B T} \right)}.\end{aligned}\quad (4)$$

Here $\phi(\epsilon)$ is the phase of the following complex function:

$$G_{hp}^A(-\epsilon)G_{hp}^R(\epsilon) - G_{hh}^A(-\epsilon)G_{pp}^R(\epsilon) = \rho(\epsilon)\exp[i\phi(\epsilon)], \quad (5)$$

where the retarded and advanced hole-particle, hole-hole, and particle-particle Green's functions are defined as follows:

$$iG_{jj'}^{R,A}(t|t') \equiv \pm\Theta(\pm t \mp t')\langle\{d_j(t), d_{j'}(t')\}\rangle, \quad (6)$$

where $j, j' = \{p, h\}$ and

$$d_p \equiv d^\dagger, \quad d_h \equiv d. \quad (7)$$

The particle-hole, particle-particle, and hole-hole retarded and advanced Green's functions are found as in

Refs. [25, 32] using the Keldysh field integral [39]. After performing the standard Keldysh rotation and integrating out the Grassmann fields of the normal metallic contacts and TSs, one obtains the Green's functions as the elements of the inverse matrix of the Keldysh effective action. The retarded Green's functions are given by the following expressions:

$$G_{ij}^R(\epsilon) = \frac{g_{ij}^R(\epsilon)}{g^R(\epsilon)}, \quad (8)$$

where

$$\begin{aligned} g_{hp}^R(\epsilon) &= 2\hbar \left\{ (\epsilon^2 - \xi_{12}^2)(\epsilon^2 - \xi_{34}^2)[i\Gamma + 2(\epsilon_d + \epsilon)] - 4(\epsilon^2 - \xi_{34}^2)[\epsilon(|\eta_1|^2 + |\eta_2|^2) + 2\xi_{12}|\eta_1||\eta_2|\sin(\Delta\phi_{12})] \right. \\ &\quad \left. - 4(\epsilon^2 - \xi_{12}^2)[\epsilon(|\eta_3|^2 + |\eta_4|^2) + 2\xi_{34}|\eta_3||\eta_4|\sin(\Delta\phi_{14} - \Delta\phi_{13})] \right\}, \\ g_{pp}^R(\epsilon) &= 8\hbar\epsilon[(\eta_1^2 + \eta_2^2)(\xi_{34}^2 - \epsilon^2) + (\eta_3^2 + \eta_4^2)(\xi_{12}^2 - \epsilon^2)], \\ g_{hh}^R(\epsilon) &= 8\hbar\epsilon[(\eta_1^{*2} + \eta_2^{*2})(\xi_{34}^2 - \epsilon^2) + (\eta_3^{*2} + \eta_4^{*2})(\xi_{12}^2 - \epsilon^2)], \\ g^R(\epsilon) &= -(\xi_{12}^2 - \epsilon^2)(\xi_{34}^2 - \epsilon^2)[4\epsilon_d^2 + (\Gamma - 2i\epsilon)^2] + 64(\epsilon^2 - \xi_{34}^2)|\eta_1|^2|\eta_2|^2\sin^2(\Delta\phi_{12}) \\ &\quad + 64(\epsilon^2 - \xi_{12}^2)|\eta_3|^2|\eta_4|^2\sin^2(\Delta\phi_{14} - \Delta\phi_{13}) + 8(\xi_{34}^2 - \epsilon^2)[\epsilon(i\Gamma + 2\epsilon)(|\eta_1|^2 + |\eta_2|^2) - 4\epsilon_d\xi_{12}|\eta_1||\eta_2|\sin(\Delta\phi_{12})] \\ &\quad + 8(\xi_{12}^2 - \epsilon^2)[\epsilon(i\Gamma + 2\epsilon)(|\eta_3|^2 + |\eta_4|^2) - 4\epsilon_d\xi_{34}|\eta_3||\eta_4|\sin(\Delta\phi_{14} - \Delta\phi_{13})] + 32\epsilon^2(|\eta_1|^2 + |\eta_2|^2)(|\eta_3|^2 + |\eta_4|^2) \\ &\quad - 128\xi_{12}\xi_{34}|\eta_1||\eta_2||\eta_3||\eta_4|\sin(\Delta\phi_{12})\sin(\Delta\phi_{14} - \Delta\phi_{13}) \\ &\quad - 32\epsilon^2 \left\{ |\eta_1|^2|\eta_3|^2\cos(2\Delta\phi_{13}) + |\eta_1|^2|\eta_4|^2\cos(2\Delta\phi_{14}) + |\eta_2|^2|\eta_3|^2\cos[2(\Delta\phi_{13} - \Delta\phi_{12})] \right. \\ &\quad \left. + |\eta_2|^2|\eta_4|^2\cos[2(\Delta\phi_{14} - \Delta\phi_{12})] \right\}. \end{aligned} \quad (9)$$

The advanced hole-particle, particle-particle, and hole-hole Green's functions are obtained from the above retarded Green's functions using the following relations:

$$\begin{aligned} G_{hp}^A(\epsilon) &= [G_{hp}^R(\epsilon)]^*, \\ G_{pp}^A(\epsilon) &= [G_{hh}^R(\epsilon)]^*, \quad G_{hh}^A(\epsilon) = [G_{pp}^R(\epsilon)]^*, \end{aligned} \quad (10)$$

which are derived from the definition of the Green's functions given in Eq. (6).

To obtain the linear conductance we calculate the current I_L in the left normal metallic contact. The rigorous derivation of this current has been done in Ref. [21] using the Keldysh field integral [39] with a proper source action specified by the current operator \hat{I}_L . This derivation is exact, general and does not depend on the number of TSs coupled to a QD. It provides an exact and general expression for the current in terms of the Green's functions whose structure (see Eqs. (8)-(10)) already depends on the number of TSs coupled to a QD. Since in the present setup the TSs are only coupled to the QD and

are not coupled to the normal metallic contacts, the exact derivation, fully identical to the one in Ref. [21], leads to the Meir-Wingreen formula [40] involving only the hole-particle Green's function. Thus, assuming $\Gamma_L = \Gamma_R$ for simplicity, the current in the left normal metallic contact is given by the following expression:

$$I_L = -\frac{e\Gamma}{4\pi\hbar^2} \int_{-\infty}^{\infty} d\epsilon [f_L(\epsilon) - f_R(\epsilon)] \text{Im}[G_{hp}^R(\epsilon)]. \quad (11)$$

Note, had the TSs been directly coupled also to the normal metallic contacts, the expression for the current in the left normal metallic contact would have been different from Eq. (11). This difference would have been expressed in additional terms such as the direct and crossed Andreev terms as is the case in setups [41–43] where a TS is directly coupled to normal metallic contacts. However, when TSs do not couple directly to normal metallic contacts, as is the case in the present setup, the direct and crossed Andreev terms do not appear.

We emphasize once again that Eq. (11) is an exact result which does not depend on the number of TSs and how their MBSs are coupled to a QD. The dependence on the number of TSs and on the coupling of their MBSs to a QD is exactly taken into account in the structure of the Green's functions, Eqs. (8)-(10). This result is a consequence of the fact that, as mentioned above, in the present setup the TSs are only coupled to the QD and are not coupled to the normal metallic contacts. As a result, the current operator \hat{I}_L specifying the source action (see Ref. [21] or many other papers, for example, Ref. [11]) does not change its form when more TSs are involved to couple via their MBSs only to the QD.

In Eq. (11) $f_{L,R}(\epsilon)$ are the Fermi-Dirac distributions of the left and right normal metallic contacts,

$$f_{L,R}(\epsilon) = \frac{1}{\exp\left[\frac{\epsilon - \mu_{L,R}}{k_B T}\right] + 1} \quad (12)$$

where

$$\mu_{L,R} = \mu \pm eV/2 \quad (13)$$

and V is the bias voltage. As mentioned above, the QD energy level ϵ_d with respect to the chemical potential μ may be tuned by a gate voltage and, as in Ref. [32], values of ϵ_d are specified with reference to μ .

We also note that in Eq. (11) one traditionally assumes that for QD setups the density of states in the normal metallic contacts is energy independent in the range of relevant energies [39]:

$$\nu_C(\epsilon) \equiv \sum_k \delta(\epsilon - \epsilon_k) \approx \frac{1}{2} \nu_c. \quad (14)$$

The linear conductance G is a quantum transport observable whose behavior is fully determined by the equilibrium state of the system. It is obtained as the derivative of the current I_L with respect to the bias voltage V taken at $V = 0$,

$$G \equiv \left. \frac{\partial I_L}{\partial V} \right|_{V=0}. \quad (15)$$

It is interesting to compare the mathematical structures of Eqs. (4) and (11). While the linear conductance involves only the hole-particle and only the retarded Green's function and only its imaginary part, the entropy involves the hole-particle, hole-hole and particle-particle Green's functions, both retarded and advanced as well as both their imaginary and real parts. Already this mathematical comparison shows that the entropy scans the Majorana induced properties of the system much more comprehensively than the linear conductance and thus Majorana induced entropy signatures are more reliable than signatures extracted from the linear conductance.

It is also important to note that in the present setup between the two TSs there exists in general a Majorana supercurrent flowing through the QD. However, it is not

our goal to compute this Majorana supercurrent in the present paper which only explores the entropy, the current in the left normal metallic contact and how they are correlated. One may also assume that under some conditions the Majorana supercurrent has a little impact. A derivation of the Majorana supercurrent and analysis of these conditions is a separate problem which will be explored in our future research (see also the outlook on the Majorana supercurrent in Section IV).

Using Eqs. (8)-(10), the entropy S and the linear conductance G are obtained by means of numerical calculations of the corresponding integrals.

To obtain results we will focus below on the regime

$$|\eta_1| > |\eta_2|, \quad |\eta_3| > |\eta_4|, \quad |\eta_{3,4}| > |\eta_1| \quad (16)$$

assuming that TS2 is coupled to the QD stronger than TS1 and the MBSs $\gamma_{1,3}$ are coupled to the QD stronger than the MBSs $\gamma_{2,4}$, respectively.

III. RESULTS

The dependence of the entropy on the phase difference $\Delta\phi_{13}$ in the low temperature regime is shown in Fig. 2 in polar coordinates where the distance from the center to a point on a curve is equal to the entropy and the polar angle is equal to $\Delta\phi_{13}$. The three polar circles correspond to the first Majorana entropy $S_M^{(1)} = k_B \ln(2^{\frac{1}{2}})$, Dirac entropy $S_D = k_B \ln(2)$ and second Majorana entropy $S_M^{(2)} = k_B \ln(2^{\frac{3}{2}})$. As can be seen, the entropy has two resonances located at $\Delta\phi_{13} = \Delta\phi_{14}$ and $\Delta\phi_{13} = \Delta\phi_{14} + \pi$. For the chosen regime, Eq. (16), the effect of $\Delta\phi_{12}$ consists in an insignificant variation of the magnitude of the entropy resonance and thus we put it to zero, $\Delta\phi_{12} = 0$. For $\Delta\phi_{14} = 0$ the maximum of the entropy resonance is equal to $S_M^{(2)}$. We find that the width of the entropy resonance grows when the temperature T increases. In the present low temperature regime this resonance is very narrow. Even a small deviation of $\Delta\phi_{13}$ from 0 or π results in a drop of the entropy from the Majorana value $S_M^{(2)}$ to a significantly lower one. For example, the drop from $S_M^{(2)}$ is already about 20% at the borders of the extremely narrow angular sectors shaded in red color, where $\Delta\phi_{13} \approx \delta$, $2\pi - \delta$, $\pi \pm \delta$ with $\delta = 0.013\pi$. Away from its resonance the entropy takes the topologically trivial Dirac value S_D which is observed almost in the whole angular range and, as a result, it will be detected with an extremely high probability in traditional experiments where the tunneling phases are uncontrolled. Thus we conclude that at low temperatures topologically trivial Dirac thermodynamic states are accumulated practically in the whole domain of the tunneling phases. Variations of $\Delta\phi_{14}$ from zero to a finite value do not help to induce Majorana thermodynamic states but make the situation even worse. Indeed, the dashed curve demonstrates that $\Delta\phi_{14}$ produces simultaneously two effects. First, it rotates the resonances from $\Delta\phi_{13} = 0$

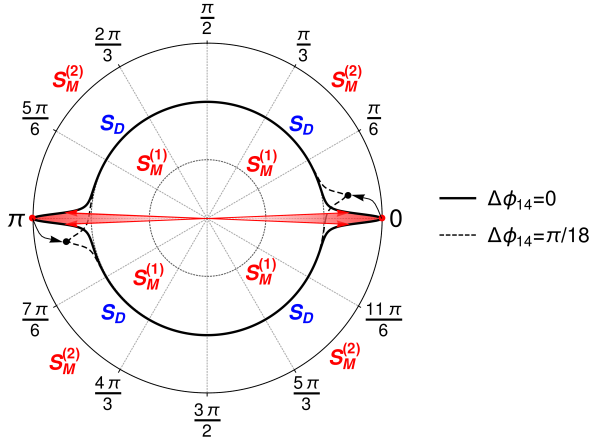


FIG. 2. Low temperature behavior of the entropy S as a function of the tunneling phase difference $\Delta\phi_{13}$ in polar coordinates. Here $k_B T/\Gamma = 10^{-5}$, $\epsilon_d/\Gamma = 10^{-1}$, $|\eta_1|/\Gamma = 10^{-2}$, $|\eta_2|/\Gamma = 5 \times 10^{-3}$, $|\eta_3|/\Gamma = 1$, $|\eta_4|/\Gamma = 4 \times 10^{-2}$, $\xi_{12}/\Gamma = 10^{-7}$, $\xi_{34}/\Gamma = 10^{-7}$. The solid curve is for $\Delta\phi_{14} = 0$ while the dashed curve is for $\Delta\phi_{14} = \pi/18$.

and $\Delta\phi_{13} = \pi$ to the new locations $\Delta\phi_{13} = \Delta\phi_{14}$ and $\Delta\phi_{13} = \Delta\phi_{14} + \pi$. Second, it suppresses the magnitude of the resonance from $S_M^{(2)}$ to a considerably smaller value which cannot be increased by variations of $\Delta\phi_{12}$ as mentioned above. These two effects are shown by the black curved arrows.

The above situation is obviously unfavorable for experimental observations of the Majorana entropy. However, it drastically changes when the temperature of this setup increases as shown in Fig. 3. As in Fig. 2, $\Delta\phi_{12} = 0$. At high temperatures the entropy has also two resonances, $\Delta\phi_{13} = \Delta\phi_{14}$, $\Delta\phi_{13} = \Delta\phi_{14} + \pi$. However, in contrast to the low temperature behavior, at high temperatures the entropy resonances have the same maximum equal to $S_M^{(2)}$ for both $\Delta\phi_{14} = 0$ and $\Delta\phi_{14} = \pi/4$. Thus we conclude that at high temperatures $\Delta\phi_{14}$ produces just a rotation of the entropy resonance. For an experimental detection of MBSs this is favorable. Indeed, at high temperatures $\Delta\phi_{14}$ does not ruin the Majorana entropy but just shifts it to new values of $\Delta\phi_{13}$ without suppressing its magnitude remaining equal to $S_M^{(2)}$. But what is much more beneficial is that due to its growth with the temperature T , the width of the entropy resonance becomes very wide. In other words, at high temperatures topologically nontrivial Majorana thermodynamic states with the entropy $S_M^{(2)}$ are accumulated in huge angular sectors of the tunneling phases. As a result, the Majorana entropy $S_M^{(2)}$ may be observed in experiments with two more advantages. First, it can be detected at very high temperatures essentially simplifying experimental observations. Second, it can be measured in conventional experiments having no specific control of the tunneling phases. Indeed, due to the accumulation of topologically nontrivial Majorana thermodynamic states

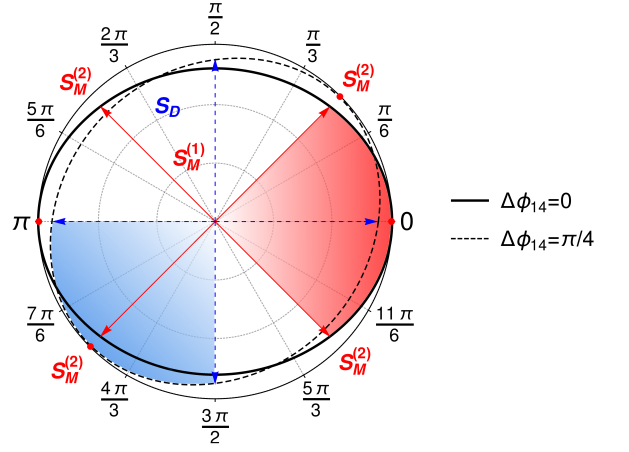


FIG. 3. High temperature behavior of the entropy S as a function of the tunneling phase difference $\Delta\phi_{13}$ in polar coordinates. Here $k_B T/\Gamma = 10^{-2}$. The other parameters have the same values as in Fig. 2. The solid curve is for $\Delta\phi_{14} = 0$ while the dashed curve is for $\Delta\phi_{14} = \pi/4$.

in vast angular domains, the dependence of the entropy on the tunneling phases becomes almost irrelevant. For example, the drop from the Majorana value $S_M^{(2)}$ is only 7% at the borders of the red and blue shaded angular sectors and their π -rotated paired sectors built around the resonance centers for the solid and dashed curves, respectively. The borders of the red shaded angular sector and its π -rotated paired sector centered for the solid curve around, respectively, 0 and π are shown by the red solid arrows, $\Delta\phi_{13} = \pi/4, 7\pi/4, 3\pi/4, 5\pi/4$. The borders of the blue shaded angular sector and its π -rotated paired sector centered for the dashed curve around, respectively, $5\pi/4$ and $\pi/4$ are shown by the blue dashed arrows, $\Delta\phi_{13} = \pi, 3\pi/2, 0, \pi/2$.

The universality of the Majorana entropy and linear conductance is demonstrated in Fig. 4. The vertical dashed line corresponds to $\epsilon_d = \Gamma$. On the left side, where the largest energy scale is Γ , there emerges a universal behavior, one of MBSs' hallmarks. Indeed, in this regime the entropy and linear conductance do not depend on the gate voltage and remain equal to the fractional Majorana values $S_M^{(2)}$ and G_M . It is important to note that the universal regime is bounded by the contact broadening because the maximal value of $|\eta_{1,2,3,4}|$ is $|\eta_3| = \Gamma$. If the value of $|\eta_3|$ had been much larger than Γ , the universal regime would have been observed at gate voltages ϵ_d much larger than Γ . The latter situation would be, however, less realistic in experimental setups and thus we focus on the regime where Γ is the largest energy scale. The Majorana universality is actually observed even up to $\epsilon_d \approx 4\Gamma$. Nevertheless, assuming that the largest energy scale is Γ and that $\Gamma \approx \Delta$ (Δ is the induced superconducting gap), increasing ϵ_d to the region $\epsilon_d > \Gamma$ might excite quasiparticles above Δ . This in turn would drive the system away from the regime dominated by Majorana thermodynamic states and consequently screen the

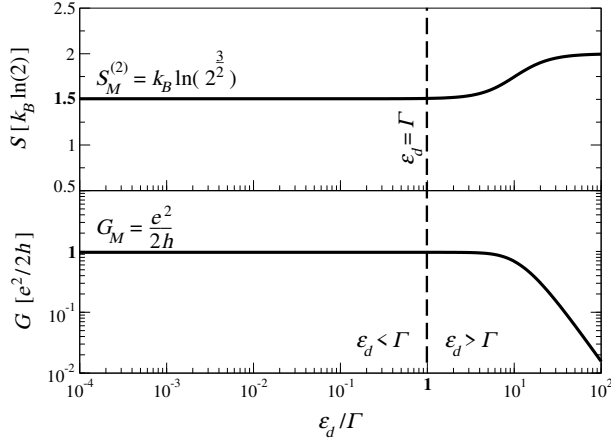


FIG. 4. The entropy S (upper panel) and linear conductance G (lower panel) as functions of the gate voltage controlling the location of the energy level ϵ_d . Here $k_B T/\Gamma = 10^{-2}$, $\Delta\phi_{13} = \pi/18$, $\Delta\phi_{14} = 0$, $\Delta\phi_{12} = 0$. The other parameters have the same values as in Fig. 2.

effect of MBSs. However, if one only considers gate voltages with $\epsilon_d \leq \Delta$, such excitations do not appear and the quantum thermodynamic and transport properties of the system are characterized by the universal fractional Majorana values $S_M^{(2)}$ and G_M . Crucially, as our numerical calculations demonstrate, in contrast to the setup in Ref. [32] with only one TS, here the second TS fully eliminates any gate voltage dependence of the tunneling phases at which the Majorana entropy is observed. This fact tremendously simplifies detections of the Majorana entropy because, in contrast to the setup with only one TS considered in Ref. [32], one does not need to rely on very sensitive adjustments between the tunneling phases and gate voltage. We have performed many numerical calculations to cover a wide range of the tunneling amplitudes, $10^{-3} \leq |\eta_{1,2,3,4}|/\Gamma \leq 1$, and from well separated MBSs, $\xi_{12}/\Gamma = \xi_{34}/\Gamma = 10^{-7}$ to significantly overlapping ones, $\xi_{12}/\Gamma = \xi_{34}/\Gamma = 10^{-2}$. In all the cases we have always reproduced the universal dependence shown in Fig. 4 without any gate voltage dependence of the tunneling phases at which the Majorana entropy is observed. This demonstrates the Majorana universality also with respect to the tunneling amplitudes $|\eta_{1,2,3,4}|$. Even when $|\eta_1| = |\eta_2| = |\eta_3| = |\eta_4| = 1$, that is outside the regime defined in Eq. (16), the Majorana entropy is observed at $\Delta\phi_{13} = \Delta\phi_{14} = 0$ which is independent of the gate voltage. However, outside the regime defined in Eq. (16) the entropy starts to strongly depend on $\Delta\phi_{13}$. Therefore, for experimental detections it is more favorable to couple one TS to the QD stronger than the second one as suggested by Eq. (16). This is not difficult to achieve via the gates controlling the values of the amplitudes $|\eta_{1,2,3,4}|$ because Eq. (16) is just an inequality and not a stringent equality and thus any fine tuning is avoided. For larger values of $\xi_{12}/\Gamma = \xi_{34}/\Gamma > 10^{-2}$ we find that the entropy is significantly reduced and goes to very small

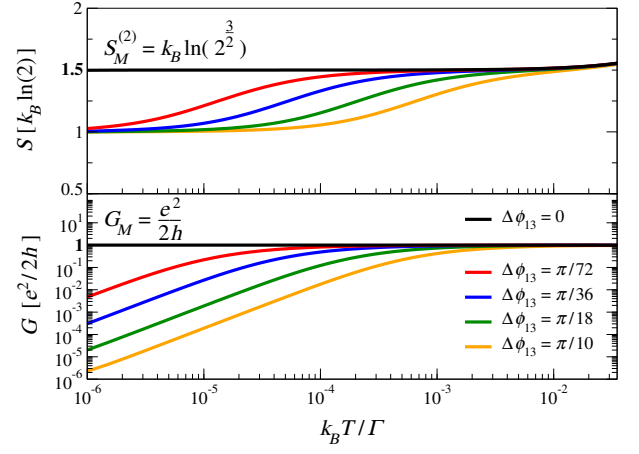


FIG. 5. The entropy S (upper panel) and linear conductance G (lower panel) as functions of the temperature T for various values of the tunneling phase difference $\Delta\phi_{13}$. Here $\Delta\phi_{14} = 0$, $\Delta\phi_{12} = 0$ and the values of the other parameters are the same as in Fig. 2.

values when $\xi_{12} = \xi_{34} = \Gamma$.

Fig. 5 shows the temperature dependence of the entropy and linear conductance. In agreement with Fig. 2, at low temperatures the entropy (upper panel) is equal to the topologically trivial Dirac value S_D for the four finite values of $\Delta\phi_{13}$ while for $\Delta\phi_{13} = 0$ it takes the topologically nontrivial Majorana value $S_M^{(2)}$. When T increases, the entropy for the finite values of $\Delta\phi_{13}$ quickly grows from S_D to the topologically nontrivial Majorana plateau $S_M^{(2)}$ extending to very high temperatures. In particular, at $k_B T/\Gamma = 3 \times 10^{-2}$ the deviation of the entropy from the fractional plateau $S_M^{(2)}$ is 2.5% for $\Delta\phi_{13} = \pi/10$. In Ref. [44] one finds $\Delta \approx 250 \mu\text{eV}$ and thus the temperature $T \approx 0.1 \text{ K}$ ($\Gamma \approx \Delta$, see above) which is very high and easily achievable in modern labs. For comparison, in the setup of Ref. [32] with only one TS the Majorana entropy $S_M^{(1)}$ is observed with similar accuracy at $T \approx 30 \text{ mK}$ as the upper limit meaning that in an experiment one could go to even lower temperatures which would be hard to achieve. The above quantum thermodynamic behavior induces striking quantum transport properties. Indeed, in accordance with common expectations, increasing T should ruin a unitary conductance maximum down to vanishing values. Here the situation is just the opposite. When T increases, there develops an accumulation of topologically nontrivial quantum thermodynamic states with the fractional Majorana entropy $S_M^{(2)}$ at finite values of $\Delta\phi_{13}$. As a result, since the linear conductance is determined by these Majorana equilibrium states, via increasing T one enhances the linear conductance (lower panel) from vanishing values at low temperatures up to the unitary fractional Majorana plateau G_M extending to very high temperatures. For example, at $k_B T/\Gamma = 3 \times 10^{-2}$ ($T \approx 0.1 \text{ K}$) the deviation of the linear conductance from the fractional Majorana plateau

G_M is 4% for $\Delta\phi_{13} = \pi/10$. At higher temperatures the deviations from the Majorana plateaus will grow as can be already seen in the upper panel.

IV. CONCLUSION

We have proposed a quantum thermodynamic approach to unambiguously detect MBSs in nanoscale systems with TSs by means of the fractional Majorana entropy. Specifically, we have revealed a remarkable phenomenon of an accumulation of Majorana thermodynamic states in wide ranges of tunneling phases via increasing the temperature T . This efficiently overcomes the problem of the low temperatures at which the Majorana entropy is detected and the problem of the sensitivity of the entropy to the tunneling phases. Moreover, involving more than two MBSs we have fully eliminated any gate voltage dependence of the Majorana entropy. As a result, the entropy becomes almost independent of the tunneling phases, does not require any fine tuning between the tunneling phases and gate voltage and its fractional Majorana value $S_M^{(2)} = k_B \ln(2^{\frac{3}{2}})$ may be detected at very high temperatures, $T \approx 0.1$ K. Since all topologically trivial zero energy bound states have integer values of the entropy, $S_n = k_B \ln(2^n)$, $n = 0, 1, 2, \dots$, a detection of the fractional entropy $S_M^{(2)}$ is a fully conclusive signature of MBSs. It has also been demonstrated how

this outstanding Majorana thermodynamic behavior induces exceptional quantum transport properties. In particular, when T increases, we have predicted an anomalous growth of the linear conductance up to the unitary fractional Majorana plateau $G_M = e^2/2h$. This shows how one can explore quantum transport using a quantum thermodynamic analysis of MBSs. Similarly, one may perform an entropy based analysis of many other equilibrium properties characterizing the system presented in this paper. For example, one may consider the Majorana supercurrent which is in general induced between the two TSs and flows through the QD. Since both the entropy and supercurrent are well defined in equilibrium, an entropic analysis of the supercurrent is a well defined problem. Additionally, how this Majorana supercurrent is correlated with the current in the left normal metallic contact, that is with the current I_L explored in this paper, is another important and interesting topic for future research on other equilibrium properties of the present setup and its generalizations to devices involving spinful quantum dots or more than two TSs modeled via more realistic Rashba nanowires.

ACKNOWLEDGMENTS

The author thanks Reinhold Egger and Sergey Frolov for valuable discussions.

-
- [1] E. Majorana, “Teoria simmetrica dell’elettrone e del positrone,” *Nuovo Cimento* **14**, 171 (1937).
 - [2] A. Yu. Kitaev, “Unpaired Majorana fermions in quantum wires,” *Phys.-Usp.* **44**, 131 (2001).
 - [3] A. Yu. Kitaev, “Fault-tolerant quantum computation by anyons,” *Ann. Phys.* **303**, 2 (2003).
 - [4] J. Alicea, “New directions in the pursuit of Majorana fermions in solid state systems,” *Rep. Prog. Phys.* **75**, 076501 (2012).
 - [5] M. Leijnse and K. Flensberg, “Introduction to topological superconductivity and Majorana fermions,” *Semicond. Sci. Technol.* **27**, 124003 (2012).
 - [6] M. Sato and S. Fujimoto, “Majorana fermions and topology in superconductors,” *J. Phys. Soc. Japan* **85**, 072001 (2016).
 - [7] R. Aguado, “Majorana quasiparticles in condensed matter,” *La Rivista del Nuovo Cimento* **40**, 523 (2017).
 - [8] R. M. Lutchyn, E. P. A. M. Bakkers, L. P. Kouwenhoven, P. Krogstrup, C. M. Marcus, and Y. Oreg, “Majorana zero modes in superconductor-semiconductor heterostructures,” *Nat. Rev. Mater.* **3**, 52 (2018).
 - [9] P. Yu, J. Chen, M. Gomanko, G. Badawy, E. P. A. M. Bakkers, K. Zuo, V. Mourik, and S. M. Frolov, “Non-Majorana states yield nearly quantized conductance in proximatized nanowires,” *Nat. Phys.* **17**, 482 (2021).
 - [10] S. Frolov, “Quantum computing’s reproducibility crisis: Majorana fermions,” *Nature* **592**, 350 (2021).
 - [11] D. E. Liu, M. Cheng, and R. M. Lutchyn, “Probing Majorana physics in quantum-dot shot-noise experiments,” *Phys. Rev. B* **91**, 081405(R) (2015).
 - [12] D. E. Liu, A. Levchenko, and R. M. Lutchyn, “Majorana zero modes choose Euler numbers as revealed by full counting statistics,” *Phys. Rev. B* **92**, 205422 (2015).
 - [13] G.-H. Feng and H.-H. Zhang, “Probing robust Majorana signatures by crossed Andreev reflection with a quantum dot,” *arXiv:2105.02830v2* (2021).
 - [14] S. Smirnov, “Non-equilibrium Majorana fluctuations,” *New J. Phys.* **19**, 063020 (2017).
 - [15] S. Valentini, M. Governale, R. Fazio, and F. Taddei, “Finite-frequency noise in a topological superconducting wire,” *Physica E* **75**, 15 (2016).
 - [16] S. Smirnov, “Majorana finite-frequency nonequilibrium quantum noise,” *Phys. Rev. B* **99**, 165427 (2019).
 - [17] M. Leijnse, “Thermoelectric signatures of a Majorana bound state coupled to a quantum dot,” *New J. Phys.* **16**, 015029 (2014).
 - [18] J. P. Ramos-Andrade, O. Ávalos-Ovando, P. A. Orellana, and S. E. Ulloa, “Thermoelectric transport through Majorana bound states and violation of Wiedemann-Franz law,” *Phys. Rev. B* **94**, 155436 (2016).
 - [19] L.-L. Sun and F. Chi, “Detecting spin heat accumulation by sign reversion of thermopower in a quantum dot side-coupled to Majorana bound states,” *J. Low Temp. Phys.* (2021).

- [20] Z.-H. Wang and W.-C. Huang, “Dual negative differential of heat generation in a strongly correlated quantum dot side-coupled to Majorana bound states,” *Front. Phys.* **9**, 727934 (2021).
- [21] S. Smirnov, “Universal Majorana thermoelectric noise,” *Phys. Rev. B* **97**, 165434 (2018).
- [22] S. Smirnov, “Dynamic Majorana resonances and universal symmetry of nonequilibrium thermoelectric quantum noise,” *Phys. Rev. B* **100**, 245410 (2019).
- [23] S. Smirnov, “Dual Majorana universality in thermally induced nonequilibrium,” *Phys. Rev. B* **101**, 125417 (2020).
- [24] K. Wrześniewski and I. Weymann, “Magnetization dynamics in a Majorana-wire-quantum-dot setup,” *Phys. Rev. B* **103**, 125413 (2021).
- [25] S. Smirnov, “Majorana tunneling entropy,” *Phys. Rev. B* **92**, 195312 (2015).
- [26] N. Hartman, C. Olsen, S. Lüscher, M. Samani, S. Fallahi, G. C. Gardner, M. Manfra, and J. Folk, “Direct entropy measurement in a mesoscopic quantum system,” *Nat. Phys.* **14**, 1083 (2018).
- [27] Y. Kleorin, H. Thierschmann, H. Buhmann, A. Georges, L. W. Molenkamp, and Y. Meir, “How to measure the entropy of a mesoscopic system via thermoelectric transport,” *Nat. Commun.* **10**, 5801 (2019).
- [28] E. Pyurbeeva and J. A. Mol, “A thermodynamic approach to measuring entropy in a few-electron nanodevice,” *Entropy* **23**, 640 (2021).
- [29] T. Child, O. Sheekey, S. Lüscher, S. Fallahi, G. C. Gardner, M. Manfra, Y. Kleorin, Y. Meir, and J. Folk, “Entropy measurement of a strongly correlated quantum dot,” *arXiv:2110.14158* (2021).
- [30] T. Child, O. Sheekey, S. Lüscher, S. Fallahi, G. C. Gardner, M. Manfra, and J. Folk, “A robust protocol for entropy measurement in mesoscopic circuits,” *arXiv:2110.14172* (2021).
- [31] E. Sela, Y. Oreg, S. Plugge, N. Hartman, S. Lüscher, and J. Folk, “Detecting the universal fractional entropy of Majorana zero modes,” *Phys. Rev. Lett.* **123**, 147702 (2019).
- [32] S. Smirnov, “Majorana entropy revival via tunneling phases,” *Phys. Rev. B* **103**, 075440 (2021).
- [33] T. Gong, X.-F. Dai, L.-L. Zhang, C. Jiang, and W.-J. Gong, “Interference effect on the Andreev reflections induced by Majorana bound states,” *J. Phys. Condens. Matter* **33**, 215303 (2021).
- [34] M. Gau, R. Egger, A. Zazunov, and Y. Gefen, “Towards dark space stabilization and manipulation in driven dissipative Majorana platforms,” *Phys. Rev. B* **102**, 134501 (2020).
- [35] M. Gau, R. Egger, A. Zazunov, and Yuval Gefen, “Driven dissipative Majorana dark spaces,” *Phys. Rev. Lett.* **125**, 147701 (2020).
- [36] S. Smirnov and M. Grifoni, “Slave-boson Keldysh field theory for the Kondo effect in quantum dots,” *Phys. Rev. B* **84**, 125303 (2011).
- [37] S. Smirnov and M. Grifoni, “Kondo effect in interacting nanoscopic systems: Keldysh field integral theory,” *Phys. Rev. B* **84**, 235314 (2011).
- [38] M. Niklas, S. Smirnov, D. Mantelli, M. Margańska, N.-V. Nguyen, W. Wernsdorfer, J.-P. Cleuziou, and M. Grifoni, “Blocking transport resonances via Kondo many-body entanglement in quantum dots,” *Nat. Commun.* **7**, 12442 (2016).
- [39] A. Altland and B. Simons, *Condensed Matter Field Theory*, 2nd ed. (Cambridge University Press, Cambridge, 2010).
- [40] Y. Meir and N. S. Wingreen, “Landauer formula for the current through an interacting electron region,” *Phys. Rev. Lett.* **68**, 2512 (1992).
- [41] X.-Q. Li and L. Xu, “Nonlocality of Majorana zero modes and teleportation: Self-consistent treatment based on the Bogoliubov-de Gennes equation,” *Phys. Rev. B* **101**, 205401 (2020).
- [42] J.-T. Ren, S.-S. Ke, Y. Guo, H.-W. Zhang, and H.-F. Lü, “Phase diagram and quantum transport in a semiconductor-superconductor hybrid nanowire with long-range pairing interactions,” *Phys. Rev. B* **103**, 045428 (2021).
- [43] N. Leumer, M. Grifoni, B. Muralidharan, and M. Margańska, “Linear and nonlinear transport across a finite kitaev chain: An exact analytical study,” *Phys. Rev. B* **103**, 165432 (2021).
- [44] V. Mourik, K. Zuo, S. M. Frolov, S. R. Plissard, E. P. A. M. Bakkers, and L. P. Kouwenhoven, “Signatures of Majorana fermions in hybrid superconductor-semiconductor nanowire devices,” *Science* **336**, 1003 (2012).